

Parking Space Detection using Textural Descriptors

Paulo Almeida, Luiz S. Oliveira
Federal University of Paraná
Department of Informatics
Curitiba, PR, Brazil - 81531-990
Email: {pauloa,lesoliveira}@inf.ufpr.br

Eunelson Silva Jr., Alceu Britto Jr., Alessandro Koerich
Pontifical Catholic University of Paraná
Graduate Program in Informatics (PPGIA)
Curitiba, PR, Brazil - 80215-901
Email: {alceu,eunelson,alekoe}@ppgia.pucpr.br

Abstract—In this paper we assess the use of textural descriptors for the problem of parking space detection. We focus our experiments on two descriptors (Local Binary Patterns and Local Phase Quantization) that have attracted a great deal of attention because of their outstanding performance in a number of applications. We show through a series of comprehensive experiments that both descriptors are able to achieve very low error rates on a database composed of 105,837 images of parking spaces. We also show that the combination of the diverse classifiers developed in this work can bring further improvement achieving an error rate of 0.16%. The results reached in this work compare favorably to other published methods.

Index Terms—intelligent transportation, vehicles, image processing, parking detection, LBP, LPQ.

I. INTRODUCTION

The impressive growth of the automotive industry allied with the lack of urban planning have caused innumerable problems in most major cities, such as traffic jam, air pollution, driver frustration and so on. Finding an empty parking space is another problem that drivers must face in most of major cities, since the cost for parking expansion is usually prohibitive, especially in large metropolitan areas. To mitigate the stress of finding an empty space in a parking lot, over the last years the industry has been developing different technologies dedicated to parking detection systems, which can be categorized into counter-based, sensor-based, and image-based [1].

Counter-based systems use sensors to count the number of vehicles entering and exiting a car park area. This can be gate-arm counters and induction loop detectors located at the entrances and exits. This kind of system can inform the total number of vacant lots in a closed car park area, but does not help much in guiding the driver to the exact location of the vacant lots. It is commonly employed in great outdoor parking lots due to its relatively low cost.

Sensor-based systems take into account detection sensors such as ultrasonic sensors which are installed at each parking space [2], [3]. This information is then relayed to display panels at strategic locations in the parking lot. The display panels provide information, direction and guide the drivers to vacant parking lots. The main drawback of the sensor-based approach is the cost for developing the system because the large amount of sensors units required to cover the entire parking lot.

The third category is based on image or video processing.

Those who advocate against the use of image-based techniques say that video cameras are remarkable expensive sensors which generate large amount of data that may be difficult to transmit over a wireless network [4]. On the other hand, the literature shows that image-based parking space detection systems can be deployed using existing surveillance cameras that are already connected to a central monitoring system [5]. It turns out that image-based systems are a good alternative for large and outdoor parking lots where the installation of hundreds or even thousands of sensors is unfeasible.

Huang and Wang [6] show that image-based systems can be classified into two categories: car-driven and space-driven. In the former, algorithms are developed to detect cars, which are the objects of interest. In this vein, there are several object detection algorithms that can be used [7], [8]. Because of the perspective distortion, observed in most images of parking lots (e.g. Figure 1) a car far away occupies a small area, hence, features few details which degrades considerably the performance of the object detection algorithms.



Figure 1: Example of a parking lot

For the space-driven, the focus lies on detecting empty spaces rather than vehicles [9], [10]. For static cameras, such as the surveillance cameras, the most used strategy is the background subtraction [11], which assumes that the variation of the background is statistically stationary within a short period. Since this hypothesis does not hold for outdoor scenes, this strategy shows rapidly its limits. A more robust approach was proposed by Sastre et al. [12] where they used Gabor filters to train a classifier with empty spaces under different light conditions.

A mix of both car- and space-driven approach has been proposed by several authors by modeling both vehicles and empty spaces using different sort of features and classification algorithms. Support Vector Machine (SVM) is certainly the most used machine learning algorithm, while color is the most employed descriptor [1], [6], [13], [14]. The performance of color-based systems, however, may be considerably affected by changes of lighting conditions. With this in mind, other families of features have been investigated, such as Edges [15], Principal Component Analysis (PCA) [5], and Optical Flow [16].

The contribution of this work is two-fold. Firstly, we introduce a database composed on 105,837 images of parking spaces captured under different weather conditions. It is available for research purposes under request¹. Secondly, we propose the use of textural descriptors to model both cars and empty spaces. Our hypothesis is that the texture pattern of a parking space is quite different from the texture of a vehicle. To validate our idea, we use two descriptors, Local Binary Patterns (LBP) and Local Phase Quantization (LPQ), that have attracted a great deal of attention because of their performance in a number of applications [17]. The concept of the LBP was first proposed by Ojala et al. in [18] as a simple approach, robust in terms of grayscale variations, which proved its ability to efficiently discriminate among a wide range of rotated textures. Later, they extended their work [19] to produce a grayscale and rotation invariant texture operator. The concept of LPQ was originally proposed by Ojansivu and Heikkila [20], and has been shown to be robust in terms of blur, and to outperform LBP in texture classification [21].

Through a set of comprehensive experiments on the proposed database, we demonstrate that the textural descriptors are a good alternative for parking detection systems. The results reported in this study show that the Support Vector Machine (SVM) classifiers trained with LBP and LPQ are able to achieve an error rate of 0.63% and 0.31%, respectively. Besides the standard versions of the LBP and LPQ, we also have tested some variations such as the LBP Rotation Invariant, LPQ with Gaussian window and LPQ Gaussian derivative quadrature filter pair. We also show that the combination of all these classifiers can further reduce the error rate to 0.16%.

II. DATABASE

The database used in this work contains 3,791 images collected from the parking lot of the Federal University of Parana, in Curitiba, Brazil. The images were acquired using a camera Microsoft LifeCam (HD-5000 USB HD) during 30 days under three different weather conditions: sunny, overcast and rainy. Rainy images contain light rain, heavy rain, and after rain. We do not have night shots since the illumination available in the parking lot was not sufficient to acquire good quality images. The resulting images were saved in JPEG color format with no compression in a resolution of 1280×720 pixels. Within the image view, there are 28 parking spaces

¹<http://web.inf.ufpr.br/vri/parking-lot1>

in total, summing up 105,847 parking spaces. Each image of the database was manually segmented into 28 parking spaces, which were labeled into occupied or empty. Roughly, 46% of them are occupied spaces, while the remaining 54% are empty spaces. Table I summarizes the database used in this work.

Table I: Summary of the parking lot database

Condition	Images	Parking Spaces	
		Occupied	Empty
Overcast	1,408	11,613	27,774
Rainy	285	2,353	5,605
Sunny	2,098	32,169	26,333
Total	3,791	46,135	59,712

Figure 2a shows an image where the 28 available spaces are marked in green. We considered as parking spaces only the spots marked on the floor. As one can notice, there are some cars parked in an unauthorized manner, i.e., in the middle of the street. Two samples of the segmented parking spaces are depicted in Figures 2b (occupied) and 2c (empty).

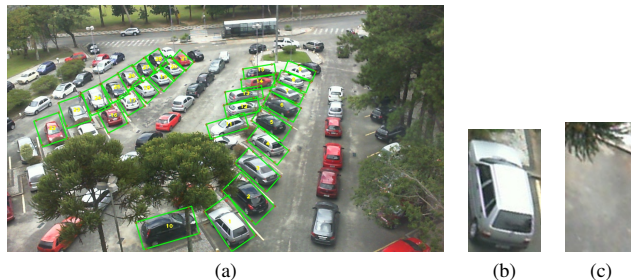


Figure 2: Segmented image: (a) 28 delimited spaces, (b) occupied sub-image, and (c) empty sub-image.

Figure 3 shows some images of the parking lot captured under the three aforementioned weather conditions: sunny, overcast, and rainy. Some challenges posed by this database can be observed from this figure. Sunny images (Figure 3a) feature overexposed cars and shadows caused by the trees. Images acquired under heavy rain (Figure 3c), on the other hand, may look like night images due the lack of natural light.

III. FEATURES

As stated before, in this paper we have used two recently developed textural descriptors that have been successfully applied into different application domains. To make this paper self-contained, in this section we briefly describe both descriptors assessed in our experiments, the Local Binary Patterns and Local Phase Quantization.

A. Local Binary Patterns

Ojala et al. [19] present a model to describe texture, called Local Binary Patterns (LBP). In this model, each pixel C contains a set of neighbors P , equally spaced at a distance R from C .

A histogram h is defined by the texture intensity differences between C and its neighbors, P . When the neighbors do

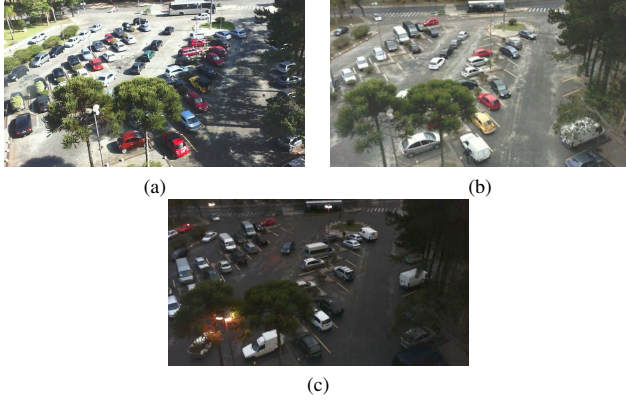


Figure 3: Images captured under different weather conditions: (a) sunny (b) overcast, and (c) heavy rain.

not correspond to an image pixel integer value, that value is obtained by interpolation. An important characteristic of this descriptor is its invariance to changes in the value of the average intensity of the central pixels, when comparing it with its neighbors.

Considering the resulting sign of the difference between C and each neighbor P , by definition, we assign a result of 1 to a positive sign, and 0 otherwise. This makes it possible to obtain the invariance of the intensity value of pixels in gray scale format. With this information, the LBP value can be obtained by multiplying the binary elements for a binomial coefficient. Therefore, a value $0 \leq C' \leq 2^P$ is generated, which is the value of the feature vector.

Observing the non uniformity of the vector obtained, Ojala et al. [19] introduced a concept based on the transition between 0s and 1s in the LBP image. They explained that a binary LBP code is considered uniform if the number of transitions is less than or equal to 2, also considering that the code is seen as a circular list. That is, the code 00100100 is not considered uniform, because it contains four transitions, while the code 00100000 is characterized as uniform, because it only has two transitions. Figure 4 illustrates this idea.

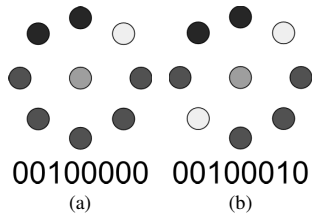


Figure 4: LBP uniform pattern [19]. (a) the two transitions showed identifies the pattern as uniform. (b) with four transitions, it is not considered a uniform pattern.

Accumulating the patterns that have more than two transitions into a single bin yields an LBP operator, denoted $LBP_{P,R}^{u2}$, with fewer than 2^P bins. For example, the number of labels for a neighborhood of 8 pixels is 256 for the standard LBP but 59

for LBP^{u2} . Then, a histogram of the frequency of the different labels produced by the LBP operator can be built [18].

LBP variants were proposed in [19]. LBP^{ri} and LBP^{riu2} have the same $LBP_{P,R}$ definition, but they have only 36 and 10 patterns, respectively. LBP^{ri} accumulates, in only one bin (Eq. 1), all binary patterns which keep the same minimum decimal value $LBP_{P,R}^{ri}$ when their P bits are rotated (ROR). LBP^{riu2} combines LBP^{u2} and LBP^{ri} definition. Thus, it uses only the uniform binary patterns and accumulates, in only one bin, those that keep the same minimum decimal value $LBP_{P,R}^{ri}$ when their P bits are rotated.

$$LBP_{P,R}^{ri} = \min\{ROR(LBP_{P,R}, i) \mid i = 0, \dots, P-1\}. \quad (1)$$

B. Local Phase Quantization

The Local Phase Quantization (LPQ) [20] is based on the blur invariance property of the Fourier phase spectrum. The local phase information of an $N \times N$ image $f(x)$ is extracted by the 2D DFT (short-term Fourier transform (STFT))

$$\hat{f}_{\mathbf{u}_i}(\mathbf{x}) = (f \times \Phi_{\mathbf{u}_i})\mathbf{x} \quad (2)$$

The filter $\Phi_{\mathbf{u}_i}$ is a complex valued $m \times m$ mask, defined in the discrete domain by

$$\Phi_{\mathbf{u}_i} = \{e^{-j2\pi\mathbf{u}_i^T \mathbf{y}} \mid \mathbf{y} \in \mathbb{Z}^2; \|\mathbf{y}\|_\infty \leq r\}, \quad (3)$$

where $r = (m-1)/2$, and \mathbf{u}_i is a 2D frequency vector. In LPQ only four complex coefficients are considered, corresponding to 2D frequencies $\mathbf{u}_1 = [a, 0]^T$, $\mathbf{u}_2 = [0, a]^T$, $\mathbf{u}_3 = [a, a]^T$, and $\mathbf{u}_4 = [a, -a]^T$, where $a = 1/m$. For the sake of convenience, the STFT presented in Eq. 2 is expressed using the vector notation presented in Eq. 4

$$\hat{f}_{\mathbf{u}_i}(\mathbf{x}) = \mathbf{w}_{\mathbf{u}_i}^T \mathbf{f}(\mathbf{x}) \quad (4)$$

where $\mathbf{w}_{\mathbf{u}}$ is the basis vector of the STFT at frequency \mathbf{u} and $\mathbf{f}(\mathbf{x})$ is a vector of length m^2 containing the image pixel values from the $m \times m$ neighborhood of \mathbf{x} .

Let

$$\mathbf{F} = [\mathbf{f}(\mathbf{x}_1), \mathbf{f}(\mathbf{x}_2), \dots, \mathbf{f}(\mathbf{x}_{N^2})] \quad (5)$$

denote an $m^2 \times N^2$ matrix that comprises the neighborhoods for all the pixels in the image and let

$$\mathbf{w} = [\mathbf{w}_R, \mathbf{w}_I]^T \quad (6)$$

where $\mathbf{w}_R = \text{Re}[\mathbf{w}_{\mathbf{u}_1}, \mathbf{w}_{\mathbf{u}_2}, \mathbf{w}_{\mathbf{u}_3}, \mathbf{w}_{\mathbf{u}_4}]$ and $\mathbf{w}_I = \text{Im}[\mathbf{w}_{\mathbf{u}_1}, \mathbf{w}_{\mathbf{u}_2}, \mathbf{w}_{\mathbf{u}_3}, \mathbf{w}_{\mathbf{u}_4}]$. In this case, $\text{Re}\{\cdot\}$ and $\text{Im}\{\cdot\}$ return the real and imaginary parts of a complex number, respectively.

The corresponding $8 \times N^2$ transformation matrix is given by

$$\hat{F} = \mathbf{wF} \quad (7)$$

In [20], the authors assume that the image function $f(x)$ is a result of a first order Markov process, where the correlation coefficient between two pixels x_i and x_j is exponentially related to their L^2 distance. Without a loss of generality, they define each pixel to have unit variance. For the vector \mathbf{f} , this leads to a $m^2 \times m^2$ covariance matrix C with elements given by

$$c_{i,j} = \sigma^{\|x_i - x_j\|} \quad (8)$$

where $\|\cdot\|$ stands for the L_2 norm. The covariance matrix of the Fourier coefficients can be obtained from

$$D = \mathbf{w}C\mathbf{w}^T \quad (9)$$

Since D is not a diagonal matrix, i.e., the coefficients are correlated, they can be uncorrelated by using the whitening transformation $E = V^T \hat{F}$ where V is an orthogonal matrix derived from the singular value decomposition (SVD) of the matrix D that is

$$D' = V^T D V \quad (10)$$

The whitened coefficients are then quantized using

$$q_{i,j} = \begin{cases} 1 & \text{if } e_{i,j} \geq 0, \\ 0 & \text{otherwise} \end{cases} \quad (11)$$

where $e_{i,j}$ are the components of E . The quantized coefficients are represented as integer values from 0-255 using binary coding

$$b_j = \sum_{i=0}^7 q_{i,j} 2^i \quad (12)$$

Finally, a histogram of these integer values from all the image positions is composed and used as a 256-dimensional feature vector in classification.

IV. EXPERIMENTS AND RESULTS

In our experiments the database was divided into training (50%) and testing (50%). The classifier used in this work was the Support Vector Machine (SVM) introduced by Vapnik in [22]. Normalization was performed by linearly scaling each attribute to the range $[-1,+1]$. The free parameters of the system and for SVM training were chosen using 5-fold cross validation. Various kernels were tried, and the best results were achieved using a Gaussian kernel. Parameters $cost$ and γ were determined through a grid search. The Overall Error Rate that we used for evaluation purposes in this work is given by Equation 13. This rate is always computed on the testing set.

$$\text{Overall Error Rate} = \frac{FP + FN}{TP + TN + FP + FN} \quad (13)$$

where FP, FN, TP , and TN stand for False Positive, False Negative, True Positive, and True Negative, respectively. These

		Classifier's Decision	
		positive	negative
Class Label	positive	TP	FN
	negative	FP	TN

Figure 5: 2×2 confusion matrix.

statistics are defined in the 2×2 confusion matrix depicted in Figure 5.

One of the limitations of SVMs is that they do not work in a probabilistic framework. There are several situations where it would be very useful to have a classifier which produces a posterior probability $P(class|input)$. In our case, we are interested in estimating probabilities because we want to try different fusion strategies, like Sum, Max, Min, Average, and Median. Due to the benefits of having classifiers estimating probabilities, many researchers have been working on the problem of estimating probabilities with SVM classifiers [23], [24]. In this work, we have adopted the strategy proposed by Platt in [23].

The first part of our experiments was devoted to compare the performance of the standard LBP and LPQ. For the LBP^{u2} we tried eight neighbors and different distances, but distance one presented the best results. LPQ was also tested for different window sizes and the best results were achieved using a 3×3 -sized window. The error rates are reported in Table II

Table II: Error Rates for LBP^{u2} and LPQ

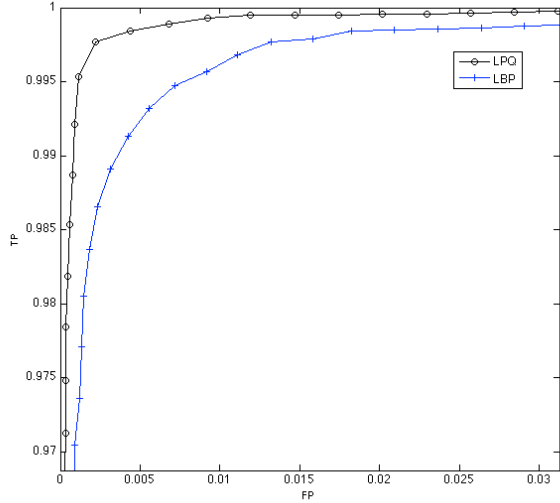
Features	Feature Vector Size	Error Rate
LBP ^{u2}	59	0.63
LPQ	256	0.31

Both classifiers achieved low error rates but the classifier trained with LPQ performed slightly better. By looking at the ROC curves (Figure 6a) and the confusion matrices (Figure 6b), we can see that LPQ reduces by half the number of False Negatives and False Positives.

The success of LBP and LPQ in several different applications instigate other researchers to further improve those descriptors. As a result of these efforts, the literature shows that some variations of LBP and LPQ achieve yet better results than the standard descriptors. With this in mind, we have assessed the LBP Rotation Invariant (LBP^{ri}) [19], LPQ STFT with Gaussian Windows and LPQ Gaussian derivative quadrature filter pair [17]. Figure 7a compares these three classifiers while Figure 7b presents their respective confusion matrices.

Observing Figure 7 it is clear that the LBP Rotation Invariant is not suitable for this task. It produced a huge error rate (8.49%) when compared to the other classifiers. Both LPQ variants, on the other hand, surpassed the LPQ with Uniform Window achieving an error rate of 0.22%.

In spite of the good results achieved so far we still can reduce the number of False Negatives and False Positives



(a)

		LBP		LPQ	
		Occupied	Empty	Occupied	Empty
Occupied		22,882	179	22,984	77
Empty		148	29,714	80	29,782

(b)

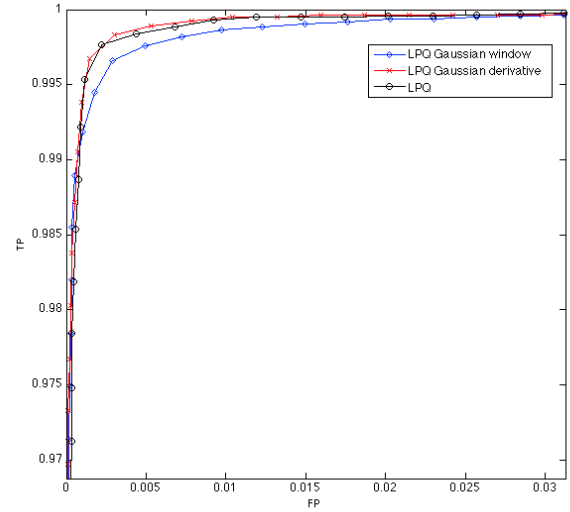
Figure 6: (a) ROC curves for LBP and LPQ classifiers for low false positive rates (b) Confusion matrices.

reported in the confusion matrices. An interesting way to do that is to profit from the diversity among the different classifiers we have built. To accomplish that, we have tried different fusion rules but the Average and Max produced the best results in all scenarios. The ROC curves and confusion matrices for the combined classifiers are depicted in Figures 8a and 8b. As one can notice, the combination was able to reduce some of the confusion and achieved an error rate of 0.16%. Table III summarizes the results of all experiments carried out in this study.

Table III: Error rates of all classifiers used in this study.

Classifier	Feature Vector Size	Error Rate (%)
LBP ^{u2}	59	0.63
LPQ	256	0.31
LBP ^{ri}	36	8.49
LPQ Gaussian window	256	0.22
LPQ Gaussian derivative	256	0.22
Fusion using Average		0.16
Fusion using Max		0.16

Comparing different works in the literature is not a straightforward task because of the lack of a common database. In spite of that, Table IV summarizes some recent works reported in the literature. Based on the results presented in this study and the performance of the related works, we can



(a)

		LBP r.i.		LPQ g.w.	
		Occupied	Empty	Occupied	Empty
Occupied		20,674	2,392	23,009	57
Empty		2,099	27,758	59	29,798

LPQ g.d.

		Occupied	Empty
Occupied		23,010	56
Empty		60	29,797

(b)

Figure 7: (a) ROC curves for LBP and LPQ classifiers (b) Confusion.

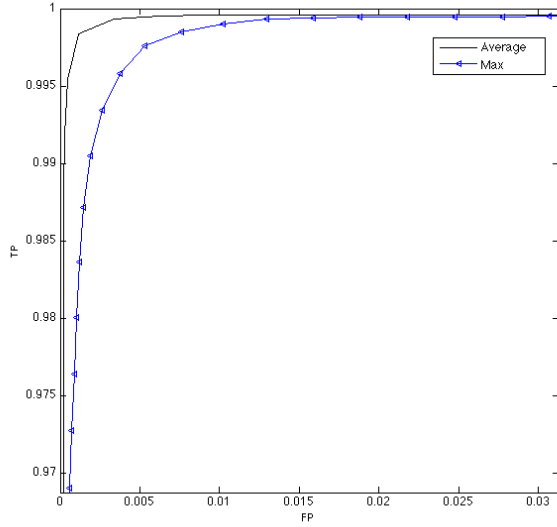
assert that textural descriptors are interesting alternatives for parking space detection problems.

Table IV: Related work reported in the literature.

Reference	Features	Number of Parking Spaces	Error rate (%)
Wu et al. [14]	Color	1,100	6.5
Sastre et al [12]	Gabor Filters	12,150	2.2
Bong et al [1]	Color	80	7.0
Wang et al [25]	Color	2,600	2.5
Ichihashi et al [5]	PCA	54,000	2.0
Huang et al [6]	Color	6,912	1.2

V. CONCLUSION

In this work we have exploited two textural descriptors for the problem of parking space detection. Our results have shown that LPQ surpassed the widely used LBP (and its variants) in all experiments. To assess such descriptors we have built a database composed of 105,837 images of parking spaces



(a)

		Average		Max	
		Occupied	Empty	Occupied	Empty
Occupied		23,006	55	23,010	51
Empty		32	29,830	46	29,816

(b)

Figure 8: (a) ROC curves for Average and Max fusion rules (b) Confusion matrices.

captured under different weather conditions. This database is available for research purposes under request.

Through our experiments, we have demonstrated that textual descriptors are a good alternative for parking space detection. Both LBP and LPQ are able to achieve very low error rates with the classifier trained with LPQ and its variants being slightly superior. Our experimental results also show that the combination of all classifiers brings some gain of performance. In such a case, the Average and Max fusion rules reached an error rate of 0.16% on the proposed database.

As future work, we intend to expand the current database by including images from other parking lots. Then, we can assess the feasibility of using a classifier trained with images of one parking lot to detect parking spaces in other parking lots that were not used during the training phase.

ACKNOWLEDGMENTES

This research has been supported by The National Council for Scientific and Technological Development (CNPq) grant 301653/2011-9.

REFERENCES

[1] D. B. L. Bong, K. C. Ting, and K. C. Lai, "Integrated approach in the design of car park occupancy information system," *IAENG International Journal of Computer Science*, vol. 35, pp. 1–8, 2008.

[2] C. Yu and J. Liu, "A type of sensor to detect occupancy of vehicle berth in carpark," in *7th International Conference on Signal Processing*, 2004, pp. 2708–2711.

[3] J. Wolff, T. Heuer, H. Gao, M. Weinmann, S. Voit, and U. Hartmann, "Parking monitor system based on magnetic field sensors," in *IEEE Conference on Intelligent Transportation Systems*, 2006, pp. 1275–1279.

[4] V. W. S. Tang, Y. Zheng, and J. Cao, "An intelligent car park management system based on wireless sensor networks," in *1st International Symposium on Pervasive Computing and Applications*, 2006, pp. 65–70.

[5] H. Ichihashi, A. Notsu, K. Honda, T. Katada, and M. Fujiyoshi, "Vacant parking space detector for outdoor parking lot by using surveillance camera and FCM classifier," in *IEEE International Conference on Fuzzy Systems*, 2009, pp. 127–134.

[6] C. C. Huang and S. J. Wang, "A hierarchical bayesian generation framework for vacant parking space detection," *IEEE Trans. ON Circuits and Systems for Video Technology*, vol. 20, pp. 1770–1785, 2010.

[7] H. Schneiderman and T. Kanade, "Object detection using the statistics of parts," *International Journal of Computer Vision*, vol. 56, pp. 151–177, 2004.

[8] P. Viola and M. Jones, "Robust real-time face detection," *International Journal of Computer Vision*, vol. 57, pp. 137–154, 2004.

[9] S. Funck, N. Mohler, and W. Oertel, "Determining car-park occupancy from single images," in *IEEE Intelligent Vehicles Symposium*, 2004, pp. 325–328.

[10] C. H. Lee, M. G. Wen, C. C. Han, and D. C. Kuo, "An automatic monitoring approach for unsupervised parking lots in outdoor," in *IEEE International Conference on Security Technology*, 2004, pp. 271–274.

[11] T. Horparasert, D. Harwood, and L. A. Davis, "A statistical approach for real-time robust background subtraction and shadow detection," in *IEEE International Conference on Computer Vision*, 1999, pp. 1–19.

[12] R. J. L. Sastre, P. G. Jimenez, F. J. Acevedo, and S. M. Bascon, "Computer algebra algorithms applied to computer vision in a parking management system," in *IEEE International Symposium on Industrial Electronics*, 2007, pp. 1675–1680.

[13] S. F. Lin, Y. Y. Chen, and S. C. Liu, "A vision-based parking lot management system," in *IEEE International Conference on System, Man, and Cybernetics*, 2006, pp. 2897–2902.

[14] Q. Wu, C. C. Huang, S. Y. Wang, W. C. Chiu, and T. H. Chen, "Robust parking space detection considering inter-space correlation," in *IEEE International Conference on Multimedia Expo*, 2007, pp. 659–662.

[15] Z. Bin, J. Dalin, W. Fang, and W. Tingting, "A design of parking space detector based on video image," in *9th International Conference on Electronic Measurement and Instruments*, vol. 2, 2009, pp. 253–256.

[16] W. Yu and T. Chen, "Parking space detection from video by augmenting training dataset," in *IEEE International Conference on Image Processing*, 2009, pp. 849–852.

[17] E. Rahtu, J. Heikkila, V. Ojansivu, and T. Ahonen, "Local phase quantization for blur-insensitive image analysis," *Image and Vision Computing*, vol. 30, pp. 501–512, 2012.

[18] T. Ojala, M. Pietikainen, and D. Harwood, "Comparative study of texture measures with classification based on feature distributions," *Pattern Recognition*, vol. 29, pp. 51–59, 1996.

[19] T. Ojala, M. Pietikainen, and T. Maenpa, "Multiresolution gray-scale and rotation invariant texture classification with local binary patterns," *IEEE Transactions on Pattern Analysis and Machine Intelligence*, vol. 24, no. 7, 2002.

[20] V. Ojansivu and J. Heikkila, "Blur insensitive texture classification using local phase quantization," in *Proc. Image and Signal Processing (ICISP 2008)*, 2008, pp. 236–243.

[21] V. Ojansivu, E. Rahtu, and J. Heikkila, "Rotation invariant local phase quantization for blur insensitive texture analysis," in *Int. Conference on Pattern Recognition*, 2008.

[22] V. Vapnik, *Statistical Learning Theory*. John Wiley and Sons, 1998.

[23] J. Platt, "Probabilistic outputs for support vector machines and comparisons to regularized likelihood methods," in *Advances in Large Margin Classifiers*, A. S. et al, Ed. MIT Press, 1999, pp. 61–74.

[24] P. Sollich, "Bayesian methods for support vector machines: Evidence and predictive class probabilities," *Machine Learning*, vol. 46, no. 1-3, pp. 21–52, 2002.

[25] S. J. Wang, Y. J. Chang, and C. Tsuhan, "A bayesian hierarchical detection framework for parking space detection," in *IEEE International Conference on Acoustics, Speech and Signal Processing*, 2008, pp. 2097–2100.